## University of South Carolina
# Scholar Commons

2016

# Simulation Of GaN Based MIS Varactor

Bojidha Babu
*University of South Carolina*

Follow this and additional works at: http://scholarcommons.sc.edu/etd

Part of the Electrical and Electronics Commons

SIMULATION OF GaN BASED MIS VARACTOR

by

Bojidha Babu

Bachelor of Engineering
Anna University, 2013

_____

Submitted in Partial Fulfillment of the Requirements

For the Degree of Master of Science in

Electrical Engineering

College of Engineering and Computing

University of South Carolina

2016
Accepted by:

Grigory Simin, Director of Thesis

Guoan Wang, Reader

Paul Allen Miller, Vice Provost and Interim Dean of Graduate Studies

www.manaraa.com

## DEDICATION

This work is dedicated to my parents who have been my soul support.

# ACKNOWLEDGEMENTS

First and foremost my deepest gratitude is to my advisor, Professor Grigory S. Simin who accepted me as a Masters student in his group. I always felt fortunate to have him as my research advisor. Under his guidance I have learnt a lot as an individual, carrying not only a small portion of his vast knowledge and experiences, but also his optimism and methodology in getting through obstacles, both in research and in life. I do not have words to thank him for all his support, help and guidance during my time in University of South Carolina. I would also like to thank chair of Electrical Engineering department, Professor Roger Dougal for providing me the opportunity to work for my graduate studies. I am grateful to my Master's thesis committee member Dr. Guoan Wang for his support.

Above all, I would like to thank my parents for showering me with their immense support and love throughout my life.

Finally, I would like to express my gratitude towards my friends for their endless support and encouragement and for making my stay in Columbia, SC a memorable one.

## ABSTRACT

This work deals with novel microwave switches based on III-Nitride varactors.

RF switches, power limiters and other control devices are important components of various RF systems, such as wireless modules of laptops, tablets, cell phones etc., satellites communication systems, radars, multi-band wireless and aerospace communications, phased array antennas and so worth. Traditional RF switches are fabricated using pin diodes or MEMS, Si MOSFETs or GaAs HEMTs. These devices have a number of fundamental limitations. Si or GaAs based devices suffer from a low breakdown voltage and cannot handle high RF power. Pin-diodes require large forward currents and do not allow for fast turn-on. III-Nitride heterostructures open tremendous opportunities for RF control devices due to the record high sheet electron density in the 2D channel, extremely low channel resistance, high breakdown field and excellent temperature stability. Recently, RF switches based on III-Nitride High Electron Mobility Transistors (HEMTs) have been developed and became commercially available. In this work, we studied a novel type of RF switch based on III-Nitride varactor. Unlike HEMTs, varactor uses capacitance modulation to control the flow of RF signal and offers a number of advantages over HEMTs: they allow for shorter channel, do not have gates or ohmic contacts and hence the fabrication is alignment- and anneal - free, they do not consume DC current and provide the DC block. Unlike regular varactor diodes, in this work, we analyze three-terminal varactor having independent control electrode which further enhances the switch performance. The varactor and varactor based RF switch analysis in

v

this work is done by modeling and simulation using Synopsys Sentaurus tools as well as MATLAB. Modeling approach allows obtaining device characteristics and material dependencies that are hardly achievable in experiments, such as effect of donor and acceptor traps or achievable switching time. The obtained results are compared with available experimental data.

# TABLE OF CONTENTS

# LIST OF FIGURES

# CHAPTER 1

# INTRODUCTION

## 1.1 Microwave switches

Microwave switches and control devices are key components which can be controlled electrically to pass, block and redirect electrical signals oscillating at RF frequencies (electromagnetic spectrum of 300MHz to 30GHz) [3]. They are used in wide range of applications like radar Tx/Rx modules, software defined radio systems, modern wireless communication and RF systems. Its importance continuously increases with increase in their complexity and functionality. Nowadays depending upon the different requirements of applications various device technologies of microwave switches are available for commercial use.

Microwave switching and control elements are widely used as a phase shifter in phased array technology, satellite communications, antennas, radar system, aerospace communication systems, wireless modules like laptops, tablets, phones etc. Depending on the type of application frequency range varies from few GHz to 100GHz. Switches with performance requirements are needed in various application spectrum. These requirements are dictated by the application systems they are part of, while the concept of switching remains a common factor. In this microwave switches signal routing is the main operation which includes selection of single or multiple signals to one output, selection of signal to one input, transfer switching to add or remove a device from signal path, matrix switching of inputs and outputs. Such applications require small device area,

1

low insertion loss (less than 1dB), high isolation (greater than 30dB), good linearity, high operating temperature and low/high power handling capability [1].



Figure 1.1 RF applications – satellite, radar systems,digital satellite system architecture

## 1.2 Microwave switch characteristics

Microwave switches achieve high performance in switching and control operation if they satisfy few basic conditions. First aspect is how well the switch can transfer power and it is determined by insertion loss. Second aspect is how well the switch can block power, it is measured by isolation. Insertion loss and isolation evaluate the switch performance in ON/OFF state. The amount of power lost in the ON state while transmitting a signal from input port to output port is measured as insertion loss [4]. It is expressed in dB. It is the ratio of output power delivered to the load at switch's output port and input power generated by the signal source.

$$IL \ (dB) = - (P_{out} \ (dBm) - P_{in} \ (dBm))$$

It has an effect by parasitic capacitance, resistance, inductance and conductance present in the switch. Insertion loss can be expressed via the switch S-parameters:

$$IL = -20 \ x \ log \ |S_{21} \ (ON)|$$

1

During the matched condition, s-parameter between input and output port of switch ($S_{21}$) in ON state is switch's insertion loss. Isolation is a measure of how output port is isolated from input port in OFF state. Typically good isolation should be more than 25dB and should avoid signal from leaking into the desired signal path [4]. It can be defined as

IS = -20 x log |$S_{21}$ (OFF)|

Third aspect is the maximum power the switch can transfer in ON state and it can block in OFF state, which is typically defined as point of input power where insertion loss increases by 1 dB because of the degradation of the switch at extremely high power. This is called 1 dB power compression point [3]. There are other aspects like return loss, noise and linearity. While the switch is in ON state the amount of the signal returned or reflected to source is called return loss ($S_{11}$). It should be zero (negative infinite in dB scale) which indicates a perfectly matched condition. Microwave switches have other important figures of merit like high power handling, fast switching speed, harsh environment operation and high temperature. Switch isolation degrades over the frequency range if a single series element acts as a control element. This can be eliminated by adding a shunt element [3]. During the ON state, shunt element turns OFF whereas series element remains ON. During the OFF state it is vice versa where shunt element turns ON and series element turns OFF [4].

## 1.3 Microwave switch types

Microwave switches can be divided into

- Micro Electro Mechanical System (MEMS) switches

- Solid state switches

2

MEMS switches use electrostatic induction for the physical movement of highly conducting thin membrane to turn the switch ON/OFF. It operates at broader bandwidth (DC to 40 GHz or higher) with high isolation and low insertion loss [5]. However MEMS switches do not exhibit high signal linearity and high power handling capabilities.

Solid state switches are made up of semiconductor materials in which electronic flow in the channel turns the switch ON/OFF. Such switching process can be controlled by applying positive or negative bias. These switches can be either unipolar or bipolar [5]. In bipolar device (PIN diode) both electrons and holes flow to control switching operation whereas in unipolar device either holes or electron participate in it. Few examples of unipolar device switches are CMOS (Complementary Metal Oxide Semiconductor), GaAs MESFET (Metal Semiconductor Field Effect Transistor), AlGaAs/GaAs HEMT (High Electron Mobility Transistor) and III-Nitride HEMTs. They are chosen for applications which require fast switching speed, smaller size, weight and reliability [5].



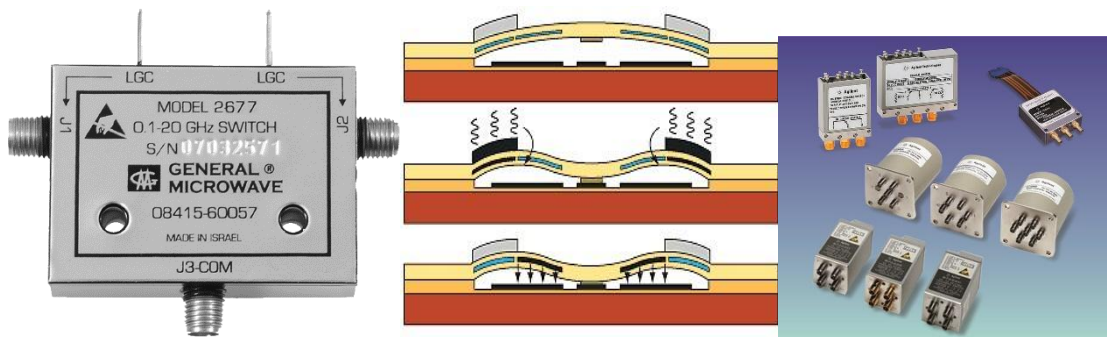Figure 1.2 RF switch-PIN diode, MEMS, solid state switches

Due to device design and inadequacies in fundamental material properties these device have performance limitations like high control voltage, self-actuation, distortions, reliability issues and low RF power. Expensive MEMS switches have limited operating life, slow switching time. On the other hand many solid state switches handles only

3

narrow bandwidth with limited operating power and linearity. PIN diodes which acts as a variable resistor at RF frequencies hold a key role in high power, high frequency applications but they have disadvantages like large size, longer switch settling time for higher power operation, require large bias current and their bipolar nature limits the device switching speed [1]. MEMS (Micro-Electro Mechanical System) operate at 0.1 to 100GHz frequencies. It offers superior performance like low insertion loss (-0.1db up to 40GHz), high isolation, low power consumption, smaller size and weight because it possess advantages of both electromechanical and semiconductor switches. But it requires improvements in high power switching, switching speed (2-40us), power handling, electrostatic discharge tolerance and reliability [1]. For low power applications, cost effectiveness and advancements in CMOS and silicon on sapphire overruns decades old GaAs MMIC. Major disadvantages of GaAs technology are low breakdown voltage, low operating temperature and cannot achieve the required linearity levels due to nature of the material.

Switching and control applications have demanding performance parameters which led to newer designs and newer materials like III-Nitrides. GaN MMICs were found to be promising candidate to replace PIN diodes and MEMS because of their low insertion loss, high isolation, fast switching speeds, high ESD tolerance and reliability.

**1.4 III Nitride RF switches**

AlGaN/GaN HFET based RF switch design facilitates as a new exemplar in microwave switching and control applications. There are numerous advantages of III-Nitride material over the other materials. GaN semiconductor material has a wide bandgap of 3.4eV. Unlike other wide bandgap material like SiC they form heterojunction

4

which is an added advantage. Past efforts in III-Nitride devices were mainly power amplifiers but many improvements in the technology resulted in elimination of surface breakdown, lower channel and contact resistance, etc.

HFET device forms 2DEG (two dimension electron gas) at the interface of the heterojunction which has very high record of sheet carrier density and electron mobility forming a metal like conducting plate [3]. This can be easily controlled to turn on or off by applying voltage to gate. They have distinctive combination of features like high breakdown voltage, higher operating temperature, robustness, chemical inertness, very high RF power, extremely low channel resistance, low off state capacitance, low insertion loss, high isolation, reliability, fast switching speed and its ability to operate as a planar structure is excellent for microwave switching and control devices [2]. In comparison with other material systems, they have high saturation current and thermal conductivity [2]. This is an ideal material for high power and high frequency applications because of its higher number in Johnson's figure of merit. Further developments in device design like insulated gate HFET (MOSHFET) enables reliability, robust RF switch with ultra-low control power and high linearity. Such RF switches can work with $10 - 100$ times higher power RF signal than compared to RF MEMS or GaAs HEMT. They are reliable and thermally stable even at cryogenic temperatures up to 300°C or higher due to their low intrinsic carrier concentration [2]. Lower power consumption and switching speed are prominent by two-three orders of magnitude when compared to PIN diodes. Thus such materials are preferred in RF systems for higher efficiency.

These III-Nitride materials exhibit strong polarization. Polarization in AlGaN/GaN heterojunction is of two types, i.e. spontaneous and piezoelectric polarization. In GaN

5

there is a difference in electronegativity between the Gallium and Nitrogen in the atomic layer which results in spontaneous polarization pointing from Ga-face to N-face. Due to difference in the lattice constants between the AlGaN and GaN layers in the heterojunction piezoelectric polarization occurs [3]. There is a mechanical strain when the AlGaN layer stretches over GaN due to which atoms are forced to shift from their electrically neutral positions giving rise to piezoelectric polarizations. Both the piezoelectric and spontaneous polarization can be oriented in the same direction by controlling the growth parameters, Al concentration and layer thickness. This enhances the total effective polarization charge which attracts the numerous free electrons at the heterojunction creating 2EG in the channel [3]. 2DEG forms a thin sheet where the concentration of electrons is really high $\sim 2 \times 10^{13}$ cm$^{-2}$. It is coupled with trapped positive charges in the AlGaN layer.

Similar to FET (Field effect transistor), AlGaN/GaN HFET is also a three terminal voltage control device. Source and drain forms ohmic contacts to 2DEG and gate terminal is a schottky contact. Current flows in the channel from source to drain contact and it is controlled by bias voltage applied to the gate terminal. DC and/or RF path is formed between input and output when a signal is applied to at the input [4]. These AlGaN/GaN HFETs generally are ON devices, even at zero gate bias the transistor is in ON state. When a negative bias is applied to the gate the net negative charge on the gate electrode starts depleting the channel under it. Typical threshold values of HFETs are -4V [4]. If the applied negative gate voltage is less than the device threshold voltage ($V_g < V_{th}$) then the channel under the gate electrode is completely depleted. This depletion indicates that the signal path is completely cut off which means the device is said to be in OFF

6

state and it starts behaving like a capacitor. For power applications gate should be placed close to the source and for microwave switching more than one gate can be used yet geometry should be symmetrical. Conventionally the gate electrodes are schottky contacts in HFET but in order to reduce the gate leakage current the design of the device was slightly modified [4]. This led to the development of insulated gate technologies in the HFETs called metal oxide semiconductor heterojunction field effect transistor (MOSHFET) and metal insulator semiconductor heterojunction field effect transistor (MISHFET). Typical threshold values of MOSHFETs are -8V [6].
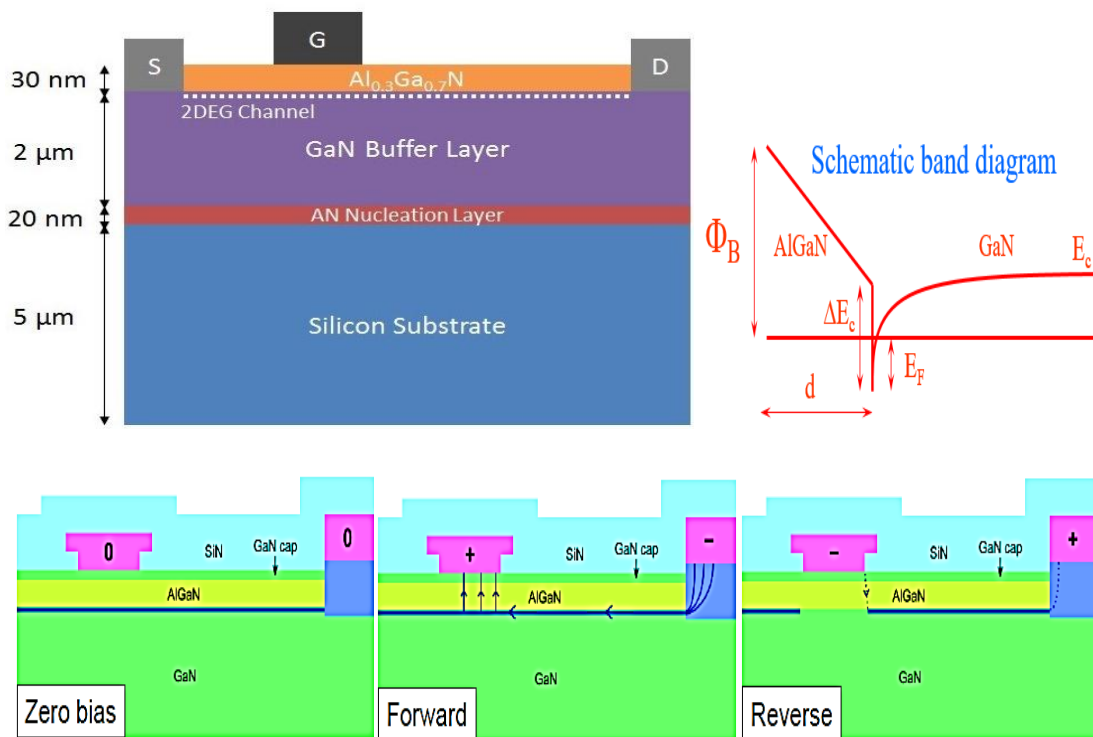
Figure 1.3 GaN HEMT structure, its band diagram and working principle representation

7

When HFETs are used as microwave switches, during ON state the channel resistance and the two contact resistance of the device are used to calculate the insertion loss whereas during OFF state the isolation is determined by the capacitance. In order to achieve efficient switch performance the product of $R_{ON}*C_{OFF}$ should be minimum [4]. ON resistance ($R_{ON}$) can be reduced only by improving growth quality and device fabrication process. Improvements in the design layout can reduce OFF capacitance ($C_{OFF}$). Research and studies demonstrate that $C_{OFF}$ decreases with increase in number of gates. Multigate device design has proven to be having maximum switching power and increased isolation.

### 1.5 Limitations of III Nitride RF HFET switches

AlGaN/GaN based HFET have two major limitations in material properties and device design which is a hindrance to further developments.

First limitation is due to material properties and it deals with ohmic contacts on the device. In AlGaN/GaN HFET source and drain (input and output) electrodes are ohmic contacts. Unlike heavy doping in Si, ohmic contact on AlGaN is formed by quickly annealing a stack of specific metal layers at very high temperature, usually at 800°C to 900°C for less than a minute [4]. AlGaN has a very wide band gap and tough chemical nature so doping is not an easy task. Rapid thermal Annealing (RTA) is a process to form ohmic contact on AlGaN. Ti layer in the metal stack plays a key role in this RTA process. At high temperature Ti anneals and react with AlGaN to form TiN clusters. This leads to the creation of N vacancies in the AlGaN layer which behave like n-type dopant to increase conductivity in the affected region. This penetration goes up to several tens of

8

nanometers and it almost reaches the heterojunction interface where the 2DEG channel is available [3]. Low temperature or short annealing is not enough for effective penetration similarly very high temperature or short annealing will destroy the 2DEG. High temperature annealing process possess limits to fabrication steps and device design. It degrades the device's morphological quality like surface roughening and area expanding which results in the increased RF resistivity and decreased critical breakdown voltage [4]. So the annealing condition is controlled carefully to achieve optimum conductivity. Ohmic contact can only be added in the beginning of the fabrication due to its high temperature requirement and also requires a separate mask [4].

Second one is due to device design and related to the gate electrode of the device. Low loss FET microwave switch needs large device periphery with multi finger structure. There exists technological challenges for the structure with long and zigzagging gate alignment. In order to maintain the device yield the gate-drain and gate-source spacing is kept above certain distance to tolerate the alignment error issue which ultimately leads to additional channel length [4]. The presence of gate leads to additional source-gate and gate-drain parasitic capacitive coupling. This occurs between RF input and output through the metal gate which limits the isolation. To avoid premature breakdown in high power switches the source-gate and gate-drain spacing is sufficiently high. This means additional channel length is included which leads to higher ON resistance and higher insertion loss. Studies have proved that existence of the gate is related to 24% of the total loss [4].

9

In the next chapter a new device design called Capacitively Coupled Contacts (C3) varactor which was introduced in order to overcome the issues with III-Nitride technology will be discussed.

# CHAPTER 2

## INTRODUCTION TO THREE TERMINAL MIS VARACTOR

### 2.1 C3 Varactor

Varactor is a voltage controlled capacitor which has variable capacitance which is a function of voltage applied across the terminals. Depending on the thickness of the depletion layer which varies with applied bias voltage the capacitance can be varied. Thickness of the depletion region is proportional to the square root of the applied voltage and the capacitance is inversely proportional to the depletion region thickness. So the capacitance is inversely proportional to the square root of the applied bias voltage.

Among the various devices using GaN technology, the varactor (voltage controlled capacitor) using 2DEG possess numerous advantages and they play a prominent role in the microwave switches and control devices. III-Nitride varactors have demonstrated high performance with significant advantages like high on/off ratio, robustness and simple gate-alignment-free technology. Our research group collectively combined the concepts of voltage controlled capacitor (varactor) in GaN based HFET switches and introduced the GaN based capacitively coupled contact ($C^3$) varactors. Capacitively coupled contact device design possess higher microwave power handling capability and low contact resistance when compared to regular HFET devices with annealed ohmic contact. This concept removes the gate from the device and reduces the overall impedance which provides higher flexibility to tune the source/drain spacing. Unlike the transistor switches where the gate is typically designed to accept only the negative bias

11

these varactor switches' device design is symmetrical so it can be designed to accept either positive or negative bias to control the device. It does not require DC current flow through the device instead it generates capacitive coupling effect between metal electrode and 2DEG to pass the microwave signal. Fig. 2.1 represents the structure of C3 switch.
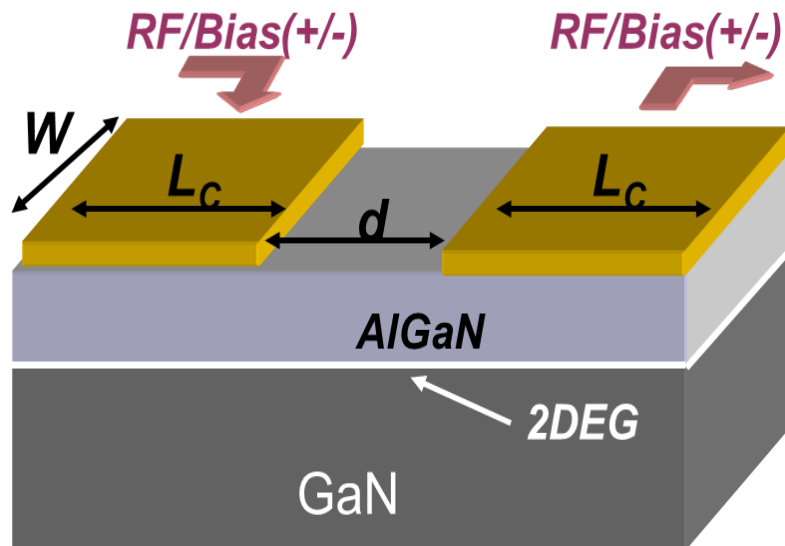


Figure 2.1 C3 varactor switch

Varactors are preferred over the field-effect transistors for the switching and RF control applications because of the few main advantages like (i) absence of the gate so the device forms short channel length as well as gate-alignment free fabrication process (ii) absence of the ohmic contacts so it eliminates annealing process and structural damage during fabrication which decreases the edge roughness and increases the breakdown voltage [4].

**Performance limitations**

$C^3$ Varactors have certain disadvantages built into the device design which affected the switch performance. When DC bias is applied between the two RF electrodes of the

$C^3$, one of the contacts turns into depletion mode and the other one into accumulation mode. This limits the OFF-capacitance and hence the achievable isolation. Regular varactors lack a separate control port, which complicates the biasing circuit and requires external circuit elements to isolate DC control from the RF path. This two terminal MIS C3 varactor has a disadvantage where the 2DEG is floating in heterostructure which is very sensitive to any parasitic crosstalk [3]. This makes it nearly impossible for fabricating the multi element switch because the potential from the other switches affect the 2DEG and makes it unstable.

## 2.2 Three-Terminal MIS Varactor with Capacitively Coupled Contacts

In order to overcome the above varactor limitations, a new device structure is proposed in this work taking advantage of the $C^3$'s bias dependent impedance. Varactor design is modified by adding a third electrode. Earlier a three terminal structure called D-MOSH was proposed but it had and additional ohmic contact as the control electrode [3]. This again involves annealing process and produces structural damage during fabrication process which decreases the edge roughness and increases the breakdown voltage.

GaN C3 varactors have highly significant leakage current when very high positive or negative bias is applied as they are conventionally designed with schottky electrodes. This leakage current limits the performance parameters. Most of the RF control devices are switches and power limiters where they are large periphery devices. In such a device or multi element IC the leakage current reaches high value at high temperature while using the varactors with schottky electrodes. In order to overcome this disadvantage Metal-Insulator-Heterostructure design was developed. This device design can be used to reduce the varactor leakage current dramatically but the earlier published works reported

13

that they have hysteresis and trapping effects. These effects compromised the performance parameters which affected the fast switching factor. Fig. 2.2 represents the structure of MIS varactor.
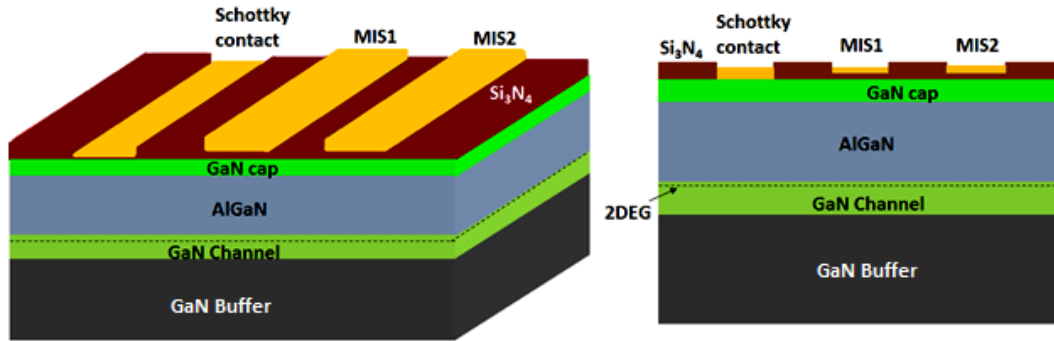


Figure 2.2 Structure of MIS varactor

The new design includes a pair of MIS contacts and one Schottky electrode (shown in the figure). This design is advantageous compared to regular varactor as explained below Unlike the RF power amplifiers and many other RF systems, RF switches do not require DC current flowing between the input and output ports. This enables more flexibility in the switch design. The C3 varactor utilizes the concept of capacitive coupling (a built in DC block) between the MIS electrodes and the channel beneath to inject RF signal into the active region. In this device, metal electrodes are deposited on top of a thin dielectric layer (5nm-10nm) which is placed on the GaN surface which forms the MIS contacts. This passivation layer reduces potential leakage current when MIS contact is under heavy bias voltage. Schottky contact is placed on the GaN surface directly. This device does not need annealing process to deposit the ohmic metal contacts resulting in much lower edge roughness which further increases the breakdown voltage. The 2DEG channel is

14

modulated with bias and through the movement of free electrons in the channel, the RF signal is passed from one contact to other. Bias can be applied to either the schottky contact or the MIS contacts. In order to deplete the channel under the MIS contacts either positive bias is applied to schottky contact or negative bias is applied to the MIS contacts. Applying bias creates a negative potential difference between MIS contacts and 2DEG channel and when the applied bias goes beyond the threshold voltage it results in depleting the channel. In this way the region under both the MIS contacts are depleted unlike $C^3$ structure. A RF signal path (active region) is set between the two MIS contacts and the schottky control electrode is placed outside this RF path so that it does not affect the insertion loss or isolation which acts similar to a gate contact in the conventional HFET. Even when a large bias is applied, the active region potential under the MIS contact remains constant. This reduces the risk of device breakdown under OFF-state and when there is high signal drop across the switch. The distance between the schottky control electrode and the MIS contacts (switch's active region) does not affect the device performance, so the schottky contact need not be necessarily placed near the MIS contacts and therefore the device does not require accurate alignment. Absence of gate has a greater impact on the channel length. The total channel length is more than two times smaller than in the HFET designed for the same breakdown voltage. This small channel length makes the resistive part of the MIS impedance is so low (1ohm x mm) than a typical HFET device whereas the capacitive part is compensated by matching the circuit. Thus MIS Varactor is a simple, robust, anneal-free, alignment-free fabrication technology and offers high yield which is compatible with power amplifiers and MMICs [4].

### 2.3 Three- terminal varactor modeling using Synopsys

In order to predict and estimate device performance, numerical simulation turns out to be a good method to understand the device physics and behavior of various parameters like voltages, doping and trap level concentrations. In this thesis a commercial simulator named Sentaurus which is provided by the company Synopsys is used. Sentaurus is a Technology Computer Aided Design (TCAD) software which aids in the process of developing and optimizing the semiconductor processing technologies and devices. It solves fundamental, physical and partial differential equations to model the structural properties and electrical behavior of a device structure. The structure is divided into series of discrete points called mesh. Simulator resolves Poisson equation, continuity equation of electrons and holes at each point of the mesh. Visualization tools are used to observe the device structure of 2D models from which various information like carrier densities, electric field, potential, energy level band gaps, geometrical structure, material type, doping concentration, electrode properties, temperature, etc. inside the device at various point of time during simulation can be studied [7].

In this MIS varactor simulation following tools were used: Sentaurus Workbench (a flexible framework environment with advanced visualization and programmability), Sentaurus Structure Editor (2D device editor), Sentaurus device (2D device simulator), and Inspect (visualizing the simulation results like one dimensional functions).

Structure of the device is defined in the following order. Initially the variables are defined in the files which are later used for the mathematical operations. Further rectangles or polygons are used to define the regions of the different materials in the

16

device structure. Electrodes are defined and placed at the edges of the device. Finally mesh is defined by creating windows in the shape of lines, rectangles or polygons.

MIS Varactor consists of one schottky electrode and two MIS electrodes. Barrier height of the schottky electrode used for this device is 0.7 eV. These electrodes are placed on top of the GaN cap layer. $Si_3N_4$ (Silicon Nitride) passivation layer of 50 nm thickness is placed on top of the GaN cap layer (except the electrodes region) to reduce the surface defects (trapping effects). For MIS contacts, $Si_3N_4$ passivation layer of 2 nm thickness is placed in between the metal and the semiconductor (GaN cap) layer. Surface pinning traps (Donor traps of 5e13 $cm^{-3}$ at an energy level of 0.4eV from the mid band gap) are defined between the passivation layer and the GaN cap layer. Electrode length and the spacing between them is assigned as 1um. Width of the device is defined as 1mm. Thickness of the top most layer GaN cap is 3 nm and its doping is 5e16 $cm^{-3}$. Below which the AlGaN spacer (2nm) and barrier layer (20nm) with a doping of 2e18 $cm^{-3}$ is placed. Polarization at the interface is larger due to which higher electron density is formed at the interface. A density gradient method is used to include the quantization of energy level in the quantum well which is formed by the band structure near the interface. This calculates a better 2DEG of 3-4nm thickness with high carrier density (1e19 $cm^{-3)}$ in the GaN channel.
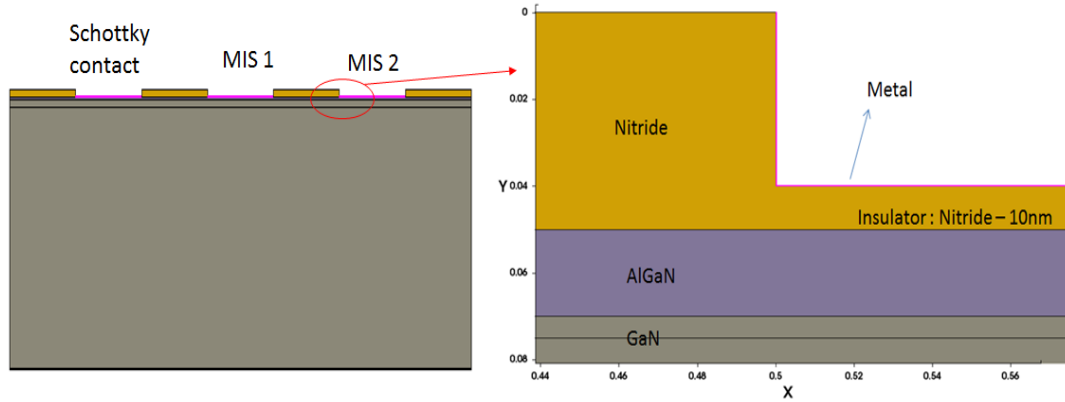
Figure 2.3 2D layout of device from Sentaurus

Al mole fraction used in the AlGaN layer is 25%. Increase in this mole fraction leads to higher polarization induced electric field which results in the rise in conduction band at the junction leading to increased electron confinement. Followed by the AlGaN layer, GaN channel and GaN buffer are defined with thickness of 0.05um and 1.95 um respectively. They have a doping of 1e14 cm$^{-3}$. At the bottom of the device an Oxide layer of 10 nm is placed.

There are several sections governing the different aspects of the simulation which are defined in the command file. Electrode section defines the type electrode, voltage bias applied and the parameters depending upon them like work function and the contact resistance. Physics section defines the models to be used in the device. There are numerous physical models which are provided by the software to define the device physics as closely as possible to the real device [7]. Various physical models like polarization, recombination, tunneling, drift - diffusion, charge distribution and density gradient were used in the simulation to emulate the MIS varactor device design. They can be defined for a specific region, material, an interface or an electrode. Traps are also

18

defined in this section. Solve sections are used to solve the numerical equations and Plot section for plotting the specifics of the quantities calculated during the simulation. Math section solves the equations in an iterative manner to converge on a solution with acceptably small error. Parameters of the materials like relative permittivity, mobility, electron and hole effective mass, electron affinity, etc. must be included in the Parameter file [7].

Simulations like transient and AC analysis were conducted in which the effect of each calibration parameter helped in understanding the various concepts in device physics. Calibration of the device is carried out to compare the performance parameters with the measured data which further concentrates to improve and optimize the performance of the device by varying the device structure.

## 2.4 Operating mechanism

MIS varactor device design is different from traditional HFET in terms of layout and operating mechanism. It has the ability to achieve high performance at high frequencies. Its simplified processing has higher yield and enhanced reliability. This novel switch based on the varactor is completely compatible with III-Nitride technology which can be integrated easily into the robust high power MMICs [3]. The key idea behind the MIS varactor is similar to C3 design where the RF control devices do not require DC current flowing through them so there is no necessity for annealed ohmic contacts for the operation. Strong capacitive coupling between the metal electrodes and highly conducting 2DEG channel is used to inject the RF signal into active region of the device [4].

19

Under small-signal assumption, sheet resistance of 2DEG channel of the MIS varactor remains constant since the signal carried by it is too small to modulate the channel. Therefore, small signal model of MIS varactor can be imagined as a periodic ladder of shunt capacitors and series resistors which represents the coupling effect and the channel resistance occurring in the MIS varactor [3]. Impedance of such model can be further explained as open-ended transmission line and it is expressed as a lossy transmission line model operating at particular RF frequency ω. At zero bias, when device is ON both the MIS electrodes have the same impedance. Series connection of the two MIS electrodes and the channel between the contacts forms the impedance of the device MIS varactor. It forms an RC transmission line between the MIS contacts and the 2DEG channel [4]. Characteristic impedance of the RC line is given by $Z_0$, propagation constant by γ and impedance by $Z_{MIS}$ [4].

$$\gamma = \sqrt{j\, 2\pi\, f\, R_{SH}\, C_{ON}}$$

$$Z_0 = \sqrt{\frac{R_{SH}}{j\, 2\,\pi\, f\, C_{ON}}}$$

$$Z_{MIS} = Z_0 \coth(\gamma L_{MIS})$$

Where f is the operating frequency, $R_{SH}$ is the sheet resistance of the channel, $C_{ON}$ is the ON-state capacitance per unit area, $L_{MIS}$ is the length of the MIS contact and W is the width of the device.

Total varactor impedance at zero bias is given by

$$Z_V = 2Z_{MIS} + R_d$$

20

$R_d = R_{SH} \times d/W$, where d is the electrode spacing

The main components of the loss in the varactor are resistive part of the contact impedance and the gap resistance. Capacitive component of the impedance is compensated by the external network circuit. So for achieving low loss condition the electrode spacing and the length must be small. In OFF state, when the bias applied to the MIS electrode exceeds the pinch off voltage the channel under the gate depletes and the channel resistance of the device becomes so small compared to the impedance so it appears to be purely capacitive.

$$Z_{MIS\_OFF} = \frac{-2j}{\omega C_{OFF}}$$

Insertion loss and isolation are calculated by the following formula

$$IL = -20 \times \log |S_{21} (ON)|$$

$$IS = -20 \times \log |S_{21} (OFF)|$$

The key parameters affecting the RF switch performance are $R_{ON}$ (resistance in the ON state) and $C_{OFF}$ (capacitance in the OFF state). HFET technology provides low sheet resistance of the 2DEG channel at the interface of the junctions. This leads to low $R_{ON}$ value with which low insertion loss is achieved. Relation between the OFF state capacitance of a MIS varactor and the $|S_{21}|$ is given by the following equations:

$$|S_{21}| = 20 \times \log_{10} |(1 + \frac{Z_{MIS_{OFF}}}{2Z_0})|$$

For a given $C_{OFF}$, with increase in frequency of operation there is an increase in $|S_{21}|$ parameter and thus it degrades the isolation.

21

Frequency dependence of the $|S_{21}|$ parameter is due to off capacitance $C_{OFF}$ since the degradation of $|S_{21}|$ in off state is purely a capacitive effect.

To summarize the third electrode on the MIS varactor (i) opens up an opportunity to use positive bias by applying it to additional Schottky electrode and DC grounding the MIS electrodes, (ii) reduces the off-capacitance nearly two times by making both MIS electrodes depleted and (iii)it eliminates the floating potential of 2DEG. Thus three terminal MIS varactor overcomes the disadvantages of two terminal varactor. Next chapter further deals with the CV dependencies, study of trap's behavior and its effects on MIS Varactor.

# CHAPTER 3

# MIS VARACTOR AS A RF SWITCH AND ITS C-V CHARACTERISTICS

## 3.1. Ideal C3 varactor over AlGaN/GaN heterostructure

Capacitance-Voltage dependencies are important characteristics of semiconductor materials as well as of many semiconductor devices. It is an easy, quick, accurate and nondestructive characterization method. In many cases the C-V plots can be directly associated with the impurity profile of the semiconductor device because the width of the depleted space charge region depends upon the applied bias and on the impurity concentration in it.

In varactors, the C-V dependence is the main device operating characteristic. The capacitance change with the applied voltage can be used either for changing the circuit resonance frequency to build electronically tuned filters and other frequency selective circuits or to change the RF impedance to make RF switches. Varactor diode can be made as a Metal-Insulator-Semiconductor diode over 2DEG channel; this allows obtaining varactor diodes fully compatible with HEMT technology and hence fabricating various multi-functional ICs.

As explained in the previous chapters, the MIS varactor studied in this work, consists of two MIS contacts and a Schottky control electrode all deposited over a planar

AlGaN/GaN heterostructure which possess 2DEG channel at the hetero interface. Representation of MIS varactor is shown in Fig. 3.1.
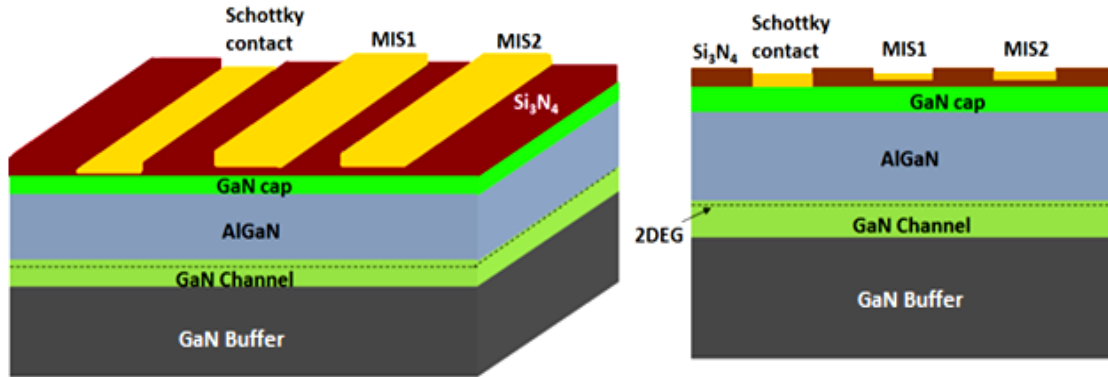


Figure 3.1 Representation of MIS varactor structure

At zero bias between the MIS electrodes, the varactor capacitance consists of two relatively large capacitances between metal electrode and the 2DEG channel connected in series. In each of these capacitances, the insulator consists of a layer dielectric material (e.g. $Si_3N_4$) deposited over AlGaN layer. Negative bias applied between the metal and the 2DEG channel depletes the 2DEG. At very large negative bias voltage, the 2DEG is fully depleted and the capacitance drops to a very low value within a small voltage range where the depletion region penetrates deeply into the device. The voltage required for the transition of higher to lower capacitance completely depends upon the carrier density of 2DEG and is therefore close to the threshold voltage of the MIS-HEMT transistor. In the three-terminal varactor studied in this work, instead of applying negative voltage to the MIS electrode we apply positive voltage to an additional Schottky contact. Because positive voltage forward biases the Schottky contact, the voltage drop across the Schottky barrier is relatively small and hence the 2DEG acquires hence most of applied potential.

24

Therefore, if the MIS electrodes are not biased (DC-grounded), positive voltage applied to the Schottky control electrode creates a reverse bias between the MIS electrode and the 2DEG channel.
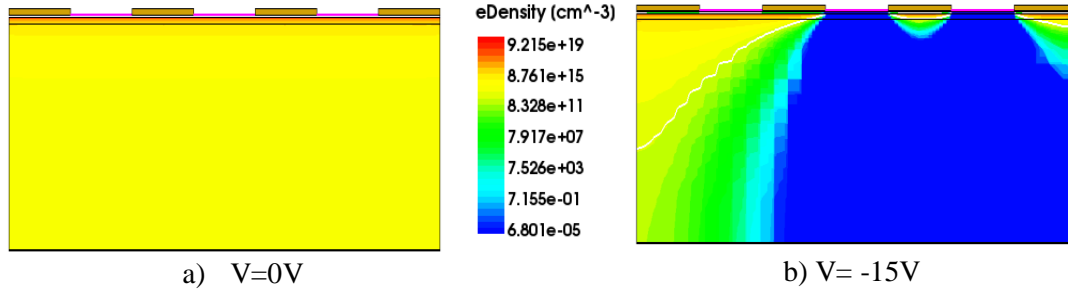


Figure 3.2 (a) snapshot of eDensity profile at zero bias (b) snapshot of eDensity profile when negative bias applied between the MIS electrodes and 2DEG channel is depleted.

As seen from the varactor structure (fig. 3.1) and the above qualitative description of its C-V dependence, in the on-state (at zero bias) the varactor capacitance can be approximated by ½ of the parallel plate capacitance formed between the metal electrode and the 2DEG. It forms an RC transmission line between the MIS contacts and the 2DEG channel. Characteristic impedance of the RC line is given by $Z_0$, propagation constant by $\gamma$ and impedance by $Z_{MIS}$ [4].

$$\gamma = \sqrt{j\, 2\pi\, f\, R_{SH}\, C_{ON}}$$

$$Z_0 = \sqrt{\frac{R_{SH}}{j\, 2\,\pi\, f\, C_{ON}}}$$

$$Z_{MIS} = Z_0 \coth(\gamma L_{MIS})$$

25

Total varactor impedance at zero bias is given by

$$Z_V = 2Z_{MIS} + R_{ON}$$

$$R_{ON} = R_{SH} \times \frac{L_{ES}}{W}$$

Where f is the operating frequency, $R_{SH}$ is the sheet resistance of the channel, $C_{ON}$ is the ON-state capacitance per unit area, $L_{ES}$ is the electrode spacing, $L_{MIS}$ is the length of the MIS contact and W is the width of the device.

However with the applied bias, when the 2DEG is partially or fully depleted, the charge distribution between the varactor MIS-electrodes becomes complicated and cannot be accurately approximated by any analytical expression. Therefore, in this work we have taken a simulation approach to obtain the C-V dependencies of the three-terminal varactor for RF switches. The simulations have been carried out using Synopsys Sentaurus device simulator.

CV simulation in Sentaurus uses the simulation of field, space charge and concentration profiles in semiconductor device coupled with small signal AC analysis. Fig 3.3 signifies the space charge and electrostatic potential profiles during the ON {a) & c)} and OFF state {b) & d)}.
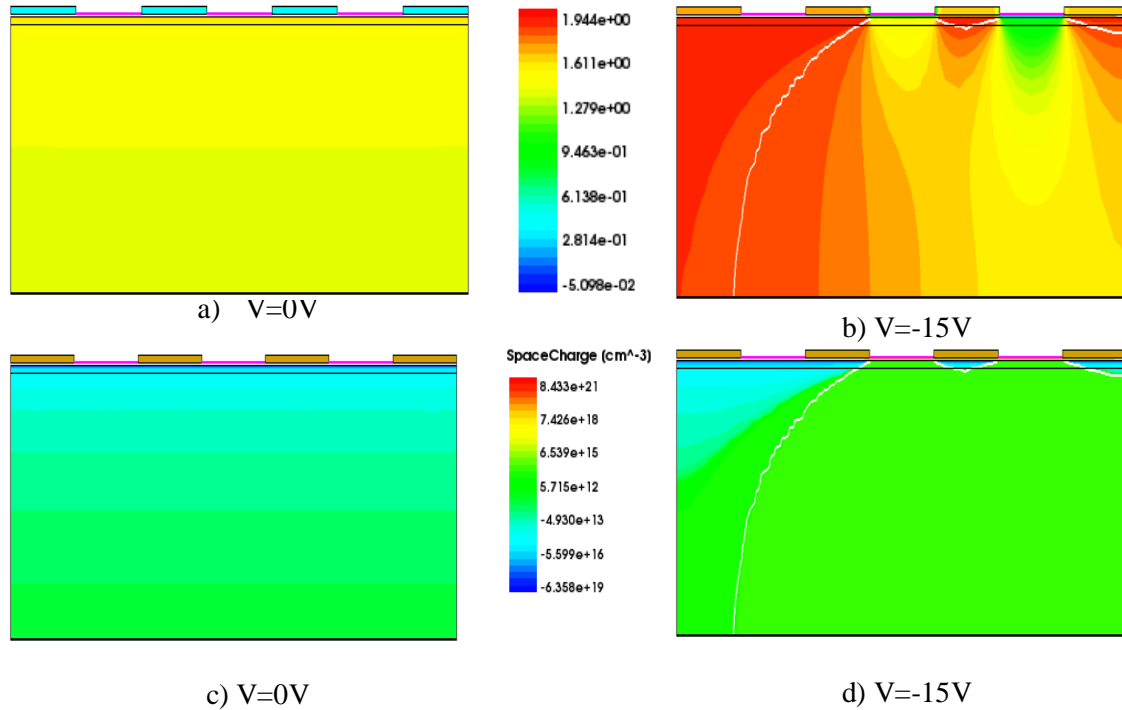
Figure 3.3 a), b) represents the electrostatic profile and c), d) represents space charge profile at different biasing conditions

An AC Coupled solve section as shown in the fig.3.4 is used with extra set of special parameters for the small signal AC analysis. It can be only used along with the mixed mode. A Node is defined along with it, for each frequency, the compact equivalent small signal model is generated. This generates a conductive-capacitive matrix. Parameters like StartFrequency, EndFrequency, NumberOfPoints, Linear and Decade are used to optimize the frequencies at which the analysis is performed as well as the frequency distribution [7]. The Exclude list removes a set of physical devices or circuit from the AC analysis. For each frequency and voltage at each node the Sentaurus creates a capacitance matrix C which can be further used to compute AC parameters such as S, H or Z [7].

27

```
15 Solve {
16        Coupled (Iterations= 10000 LinesearchDamping= 1e-5) {Poisson}
17        Coupled (Iterations= 10000 LinesearchDamping= 1e-5) {Poisson Electron Hole}
18
19        Quasistationary (
20                InitialStep= 2e-2 Minstep= 1e-5 MaxStep= 0.1    # was 0.04
21                Goal { Parameter= Vg.dc Voltage=-15}
22        ){ ACCoupled (
23        StartFrequency= 1e6 EndFrequency= 1e6 NumberOfPoints= 1 Decade
24        Node(s g1 g2) Exclude(Vs Vg Rg1 Rg2)
25          ACCompute (Time= (Range= (0 1)  Intervals= 30))
26          ){ Poisson Electron Hole }
27    Plot(FilePrefix="n@node@_0_1" Time=(0.1))
28    Plot(FilePrefix="n@node@_0_25" Time=(0.25))
29    Plot(FilePrefix="n@node@_0_5" Time=(0.5))
30    Plot(FilePrefix="n@node@_0_98" Time=(0.98))
31    }
32 }
```

Figure 3.4 AC Analysis using Sentaurus

ON capacitance is calculated using the formulae as shown below,

$$C_{ON1} = \frac{1}{(\frac{1}{C_b}+\frac{1}{C_d})} = 2.7561e\text{-}12 \text{ F}$$

Where $C_b$ and $C_d$ are the barrier and dielectric capacitance which are calculated using permittivity of the free space ($\varepsilon_0$) and the dielectric permittivity of the barrier and dielectric. OFF capacitance was measured to be as

$C_{OFF1} = 0.15e\text{-}12 \text{ F}$

These results of analytical formulas were compared with simulated CV dependencies. Fig3.5 represents the Sentaurus simulated CV plots during varying biasing conditions.
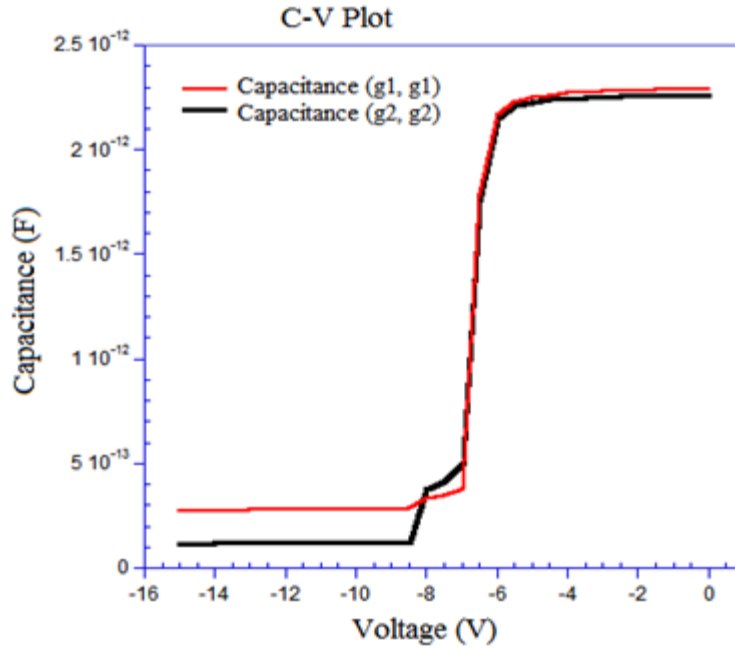
28

Figure 3.5 CV plot simulated using Sentaurus with varying bias condition

Sentaurus creates the capacitance matrix C from which the capacitance under the MIS electrode were considered for comparison with analytical values. The device ON and OFF capacitances of three terminal MIS varactor are determined from the simulated CV plot as follows.

$C_{ON}$ = 2.2e-12 F and $C_{OFF}$ = 1.16e-13 F

From earlier research works, capacitance estimated for two terminal C3 varactor by using analytical formulas is

$C_{ON}$ = 2.7561e-12 F and $C_{OFF}$ = 0.15e-12 F

29

The simulated results of three terminal MIS varactor are compared with the analytical results of the two terminal C3 varactor. The expected result of this comparison is that the ON-capacitance is close to the approximation described above (series connection of two capacitors) but the OFF capacitance is not exactly equal to simplified analytical expressions. Sentaurus simulated three terminal MIS varactor OFF capacitance is much lower than the experimentally measured two terminal OFF capacitance. This increases the Isolation. This low OFF capacitance is possible in three terminal MIS varactor because both the MIS electrodes are depleted simultaneously in the OFF state which leads to very low capacitance whereas in two terminal C3 varactor out of the two electrodes only turns OFF and the other remains ON (only one electrode is depleted and the other is accumulated). Hence the series capacitance of the two electrodes remains high which leads to higher OFF capacitance values when compared to three MIS varactor.

## 3.2. Effect of defects in AlGaN/GaN heterostructure on varactor C-V characteristics

AlGaN/GaN heterostructures typically have very high defect concentration in the GaN buffer layer. Typical measured acceptor trap concentration is approximately 1e16 cm^-3 and its energy level varies from 0.3eV to 0.5eV from conduction band [8]. This is due to the fact that these heterostructures are grown over SiC or sapphire or Si substrates, which have the lattice constant different from that of GaN. Therefore, the defect generation during the material growth and device processing is nearly inevitable. In GaN HEMTs carrier trapping by the defects is a major issue which severely limits the performance of high-speed amplifiers and power switches [8]. Current collapse is a trap related phenomenon limiting the output power which affects the device switching

30

response (a critical parameter for satellite communication). This current collapse occurs when the hot carriers are injected and trapped outside the conduction band in the GaN buffer layer. Current flowing through the transistor channel is directly affected by the traps, which in turn affects the switching range, insertion loss, isolation loss and switching time [9].

MIS varactor device uses CV dependence to achieve switching as opposed to I-Vs used in HEMT device for the same purpose. The C-V dependence is expected to be affected by traps much weaker than the I-V. Indeed, when certain amount of electrons in the 2DEG channel is trapped by the defects, the HEMT current decreases proportionally, which directly affects the gain, transconductance, insertion loss and other characteristics of the HEMT based circuits. However, the same amount of trapped carriers will not have significant effect on the C-V characteristics as long as the 2DEG still exists. We therefore expect the varactor performance to be much less vulnerable to the defects than that of HEMT.

In the presence of defects, analytically obtaining accurate electric field, electron density, space charge and other profiles in the MIS varactor is nearly impossible. We therefore have carried out the simulation of these profiles along with C-Vs of varactor in presence of defects using Synopsys Sentaurus simulations.

In the considered modeling experiments, acceptor bulk traps are used which are distributed uniformly across the GaN buffer layer. In Sentaurus, the traps are modeled with Shockley-Read-Hall recombination in the continuity equation. Acceptor trap in GaN buffer layer with different energy level from 0.3 eV to 0.5eV below the conduction band

31

were used for experiments. Varying concentration from 1e16 cm$^{-3}$ to 1e18 cm$^{-3}$ were used for each energy level to study about the behavior of traps and its effects. Cross section of 1e-15 cm$^2$ were used for the electron and hole capture cross sections which is consistent with other reported numerical simulation. In Fig. 3.6 the CV plots depicts effect of traps on the capacitance.
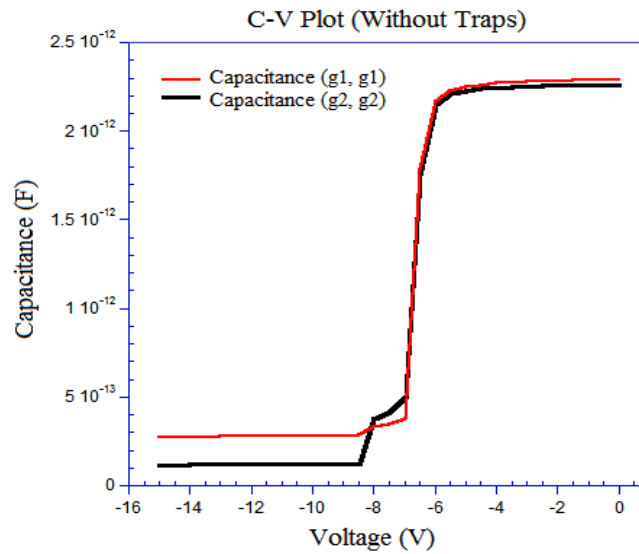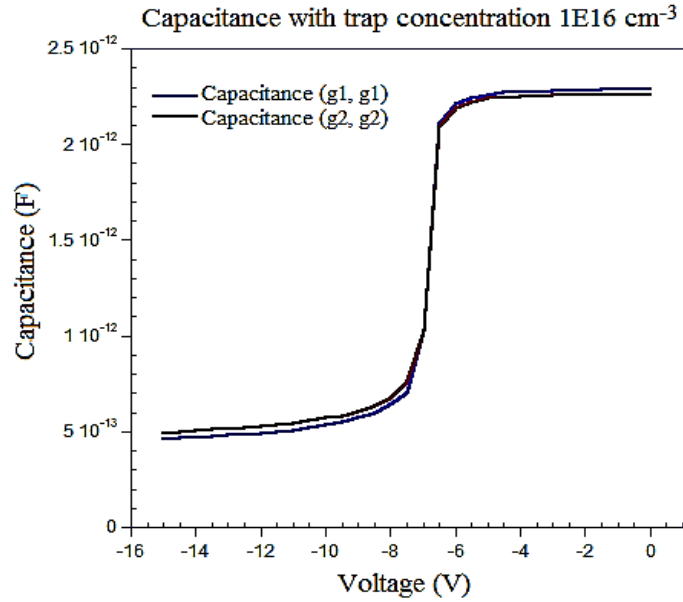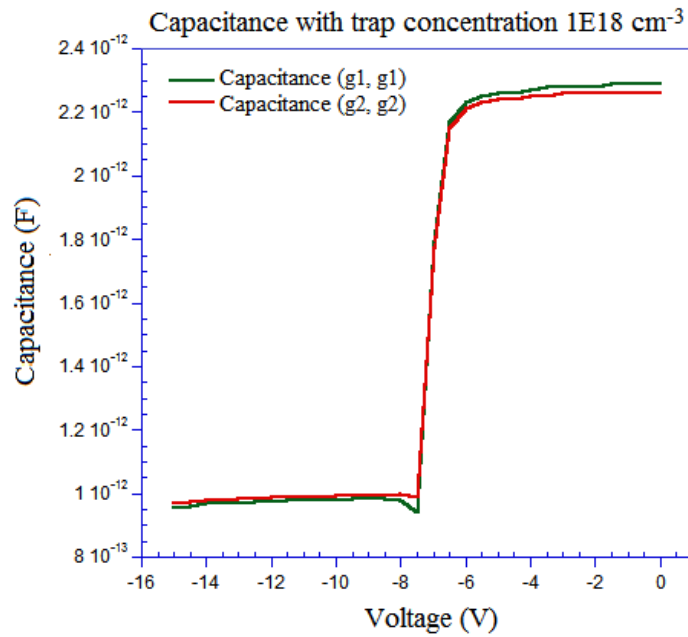


Figure 3.6 (a) CV dependencies of MIS varactor without traps (same as in Figure 3.5 - shown here for comparison)

Capacitance with trap concentration 1E16 cm$^{-3}$

(b) CV dependencies with acceptor trap concentration $10^{16}$ cm$^{-3}$.



Capacitance with trap concentration 1E18 cm$^{-3}$

(c) CV dependencies with acceptor trap concentration $10^{18}$ cm$^{-3}$; this plot corresponds to a very high defect concentration, normally not present in a decent quality heterostructures.

33

Peak capacitance or the ON capacitance values are nearly not affected by traps whereas the OFF capacitance is marginally affected by the traps. Actual effect of the traps is prominent in the eDensity profile of the device with increase in the negative bias applied to the electrodes.

For further study of traps different types of traps with various concentrations were used in simulation. Fig. 3.7 depicts effect of traps on the eDensity profile {a) & b)} MIS varactor (without traps): bias applied from 0V to -15V on the MIS electrode. {c) & d)} with acceptor traps with same biasing conditions as without traps. {e) & f)} with donor traps with same biasing conditions as without traps.
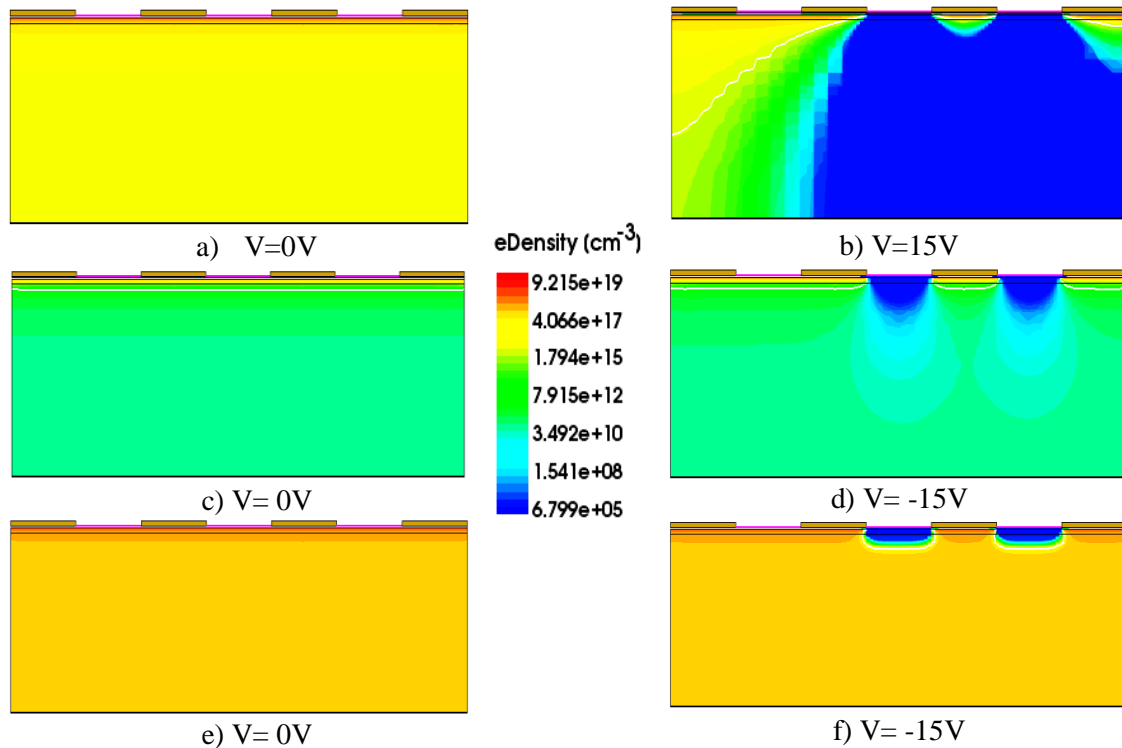


Figure 3.7{a) & b)} eDensity profile of MIS Varactor (without traps): bias applied from 0V to -15V {c) & d)} acceptor traps with same biasing conditions {e) & f)} with donor traps

34

Electrons in 2DEG channel are trapped by acceptor traps in GaN buffer layer and it is clearly observable in the eDensity profile with the varying applied bias. In transistors, changes in charge profile of 2DEG due to traps have a direct effect on the current parameter which in turn affects the switching response. MIS varactor acts as a capacitor and the capacitance value is not drastically affected when there are changes in electron density of 2DEG which is the bottom plate of the capacitor. Capacitance values have drastic changes only when the 2DEG disappears completely. To deplete the entire 2DEG at zero bias a huge concentration of traps are required which is typically not possible. So the capacitance profiles are less sensitive to the GaN buffer traps and hence switching response in MIS varactor is better than regular transistors.

## 2.5 Comparison between the Three-terminal and two-terminal varactor RF switch performance

RF performance characteristics of MIS varactor are simulated using MATLAB. Device parameters such as sheet resistance, electrode spacing and length, width, ON state and OFF state capacitance values are extracted from the Sentaurus simulation to use in the MATLAB code.

In order to provide a matched simulation results a comparison of performance parameters between the proposed three-terminal MIS varactor and studied and published earlier two-terminal C3 device is presented. A MIS varactor device was simulated in the Sentaurus software with device parameters exactly same as a C3 switch. Electrode length and the spacing between them is 2um. An additional schottky electrode with 1 um length is placed 1 um away from the MIS contacts. $W_{SER}$ and $W_{SHT}$ dimension set is chosen as 0.4mm/0.4 mm and sheet resistance as 310 ohm/sq. Negative bias voltage is applied to

MIS contacts to deplete the channel under them. Using Sentaurus $C_{ON}$ was obtained as 2.2 pF/mm and $C_{OFF}$ as 1.16e-13 F/mm. From the above design parameters we were able to get isolation of 30dB at 18 GHz for the MIS varactor without any additional compensating inductance added in the circuit whereas C3 was able to achieve only 25dB at 18 GHz.
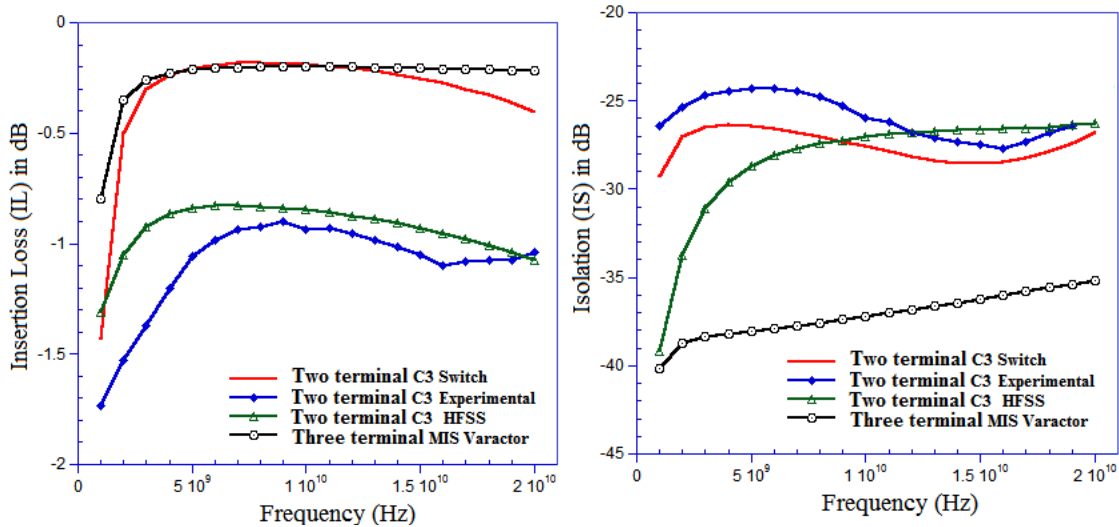


Figure 3.8 Insertion loss and isolation of the new three-terminal MIS varactor switch compared with experimental and simulated of two-terminal varactor switch.

Device parameters of a regular MIS varactor device (simulated using Sentaurus) as discussed earlier are used in MATLAB software to plot insertion loss and isolation. Different sets of series and shunt device dimensions were used to find the best dimension at fixed frequency 10 GHz.
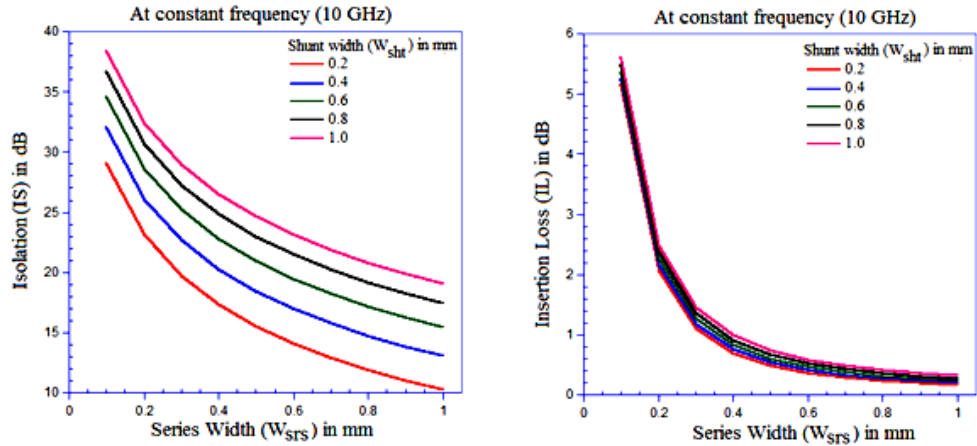
Figure 3.9 Isolation and Insertion loss variation with increasing device width

Insertion loss and isolation is plotted for different voltage bias applied to the MIS contacts. The turn off voltage is typically 6-9 V for MIS varactor [6]. Depending on the voltage applied to MIS contacts the depletion region under them varies, this also alters the electrode spacing length considered for capacitance calculation. In accordance with the Sentaurus simulation, various $C_{OFF}$ capacitance values at various voltages were used in MATLAB simulation.
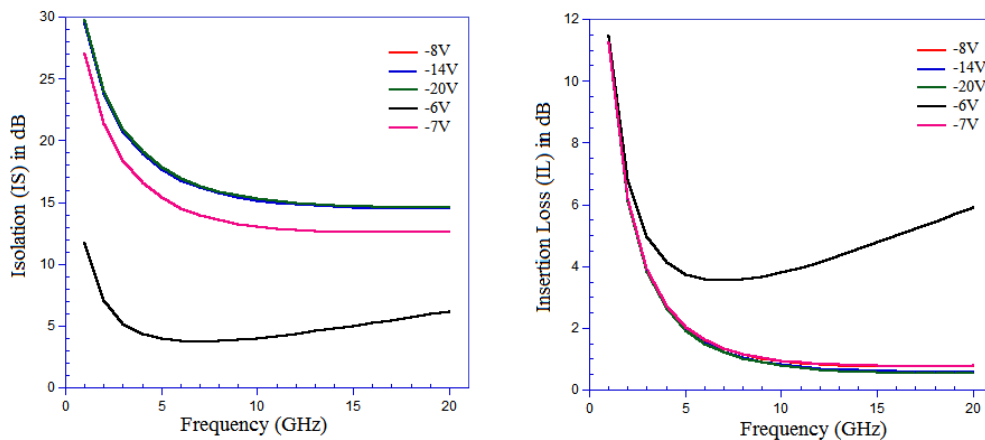


Figure 3.10 Isolation and Insertion loss with varying bias conditions

37

Trapping is the most damaging effect which limit the device performance and reliability in GaN HEMTs. Various researches take place to study its behavior and lessen its effect on devices. For comparative study, insertion and isolation loss are calculated and plotted for various conditions such as MIS varactor device without any traps (ideal case) and with different types of trap at different concentration.
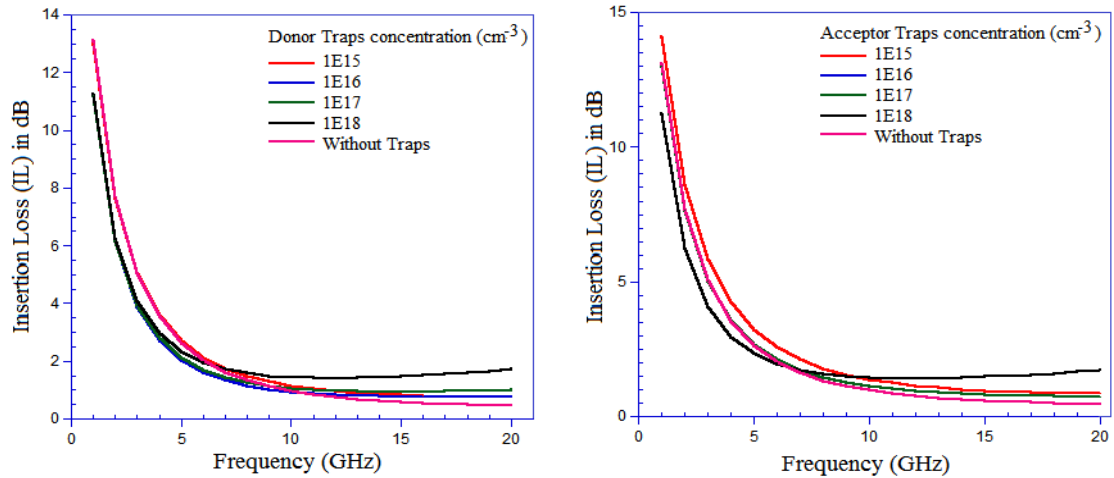


Fig. 3.11 Insertion loss with variation in different type of traps
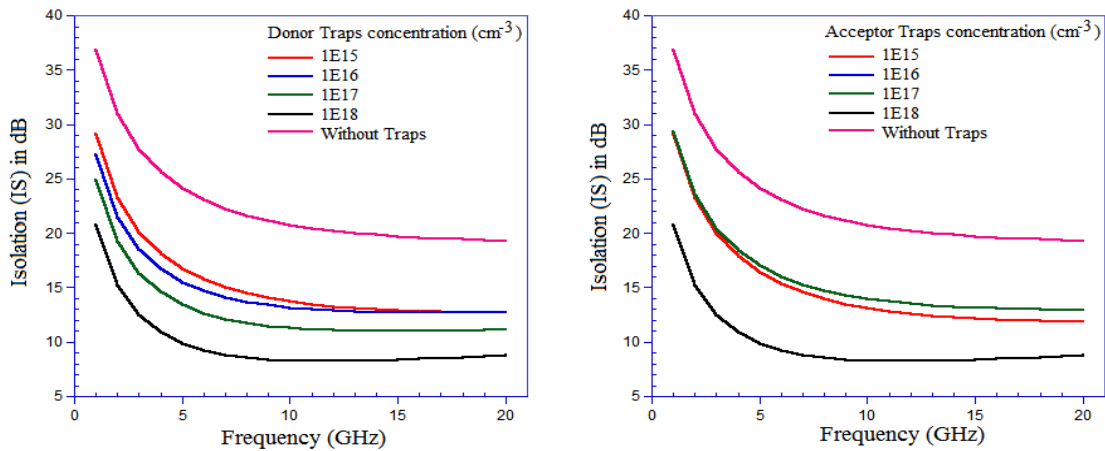


Fig. 3.12 Isolation with variation in different type of traps

To summarize, this chapter clearly explained CV and RF performance characteristics of the new three terminal MIS varactor. Its results were compared with the experimental results of the existing two terminal C3 varactor, where the Insertion loss is almost the same but the Isolation of three terminal MIS varactor is lot better. This is clearly due to the fact that the three terminal MIS varactor OFF capacitance is much lower than that of the two terminal C3 varactor.

39

# CHAPTER 4

## TRANSIENT RESPONSE OF MIS VARACTOR

### 4.1 Transient response of C3 MIS varactor

Microwave switches are used in wide range of modern electronic systems including communications systems, civilian and military radars, and electronic-warfare (EW) systems. Microwave switches can be compared in terms of many different performance parameters, although one of the clearest differentiators is switching speed. It is especially important in applications that require the stacking of multiple switches in series. For the communication between airplanes and satellites as well as for electrically steerable antennas for radar systems, highly integrated RF-front-ends with good switching speed are vital. This initiates the necessity to study the speed of response of microwave switches.

A voltage-controlled capacitor (varactor) formed over 2DEG has been shown to have high capacitance on/off ratio up to microwave frequencies, it was also suggested to be a promising switching device [4]. Therefore it is important to study the expected speed of response for MIS varactor switch to the applied bias.

40

In general transient response curves from which switching speed is depicted can be defined as follows:

- Switching speed is defined as the time needed to change the state of a switch port from ON to OFF or from OFF to ON. Switching speed is often characterized in two ways: Rise/Fall time, and ON/OFF time.

- Rise time is the time it takes for the detected RF output to raise from 10% to 90% of the final value, when a switch arm is changed from an OFF state to an ON state.

- Fall time is the time it takes for the detected RF output to drop from 90% to 10% of the initial value, when a switch arm is changed from an ON state to an OFF state.

- Rise and fall times do not include the switch delay time.

- ON time is the time period from 50% of the transition of the control signal to 90% of the detected RF output when the switch arm is changed from an OFF state (isolation) to an ON state (insertion loss).

- OFF time is the time period from 50% of the transition of the control signal to 10% of the detected RF output when the switch arm is changed from an ON state (insertion loss) to an OFF state (isolation).

- The ON and OFF times include the switch propagation delay. Switching time of an RF switch can be measured using an RF signal generator, a square law RF detector (e.g. Schottky diode), a fast Rising/Falling edge (~10nsec) square wave function (pulse) generator for switch control, and an oscilloscope

41

For a MIS Varactor which consists of two MIS contacts and a Schottky control electrode all deposited over a planar AlGaN/GaN heterostructure which possess 2DEG channel at the hetero interface. This varactor is said to be in ON state when there is zero bias between the MIS electrodes, the varactor capacitance consists of two relatively large capacitances between metal electrode and the 2DEG channel connected in series. At very large negative bias voltage, the 2DEG is fully depleted and depletion region penetrates deeply into the device where the capacitance drops to a very low value. This state is termed as OFF state. Switching response of this varactor is studied using Sentaurus. Representation of the MIS varactor structure is shown in the Fig 4.1.
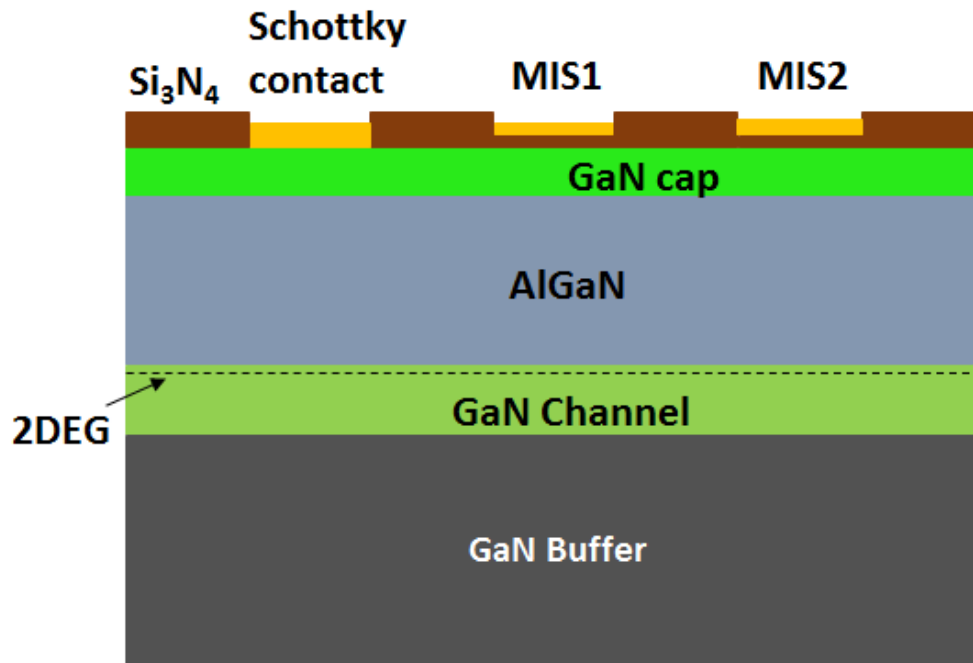


Figure 4.1 2D MIS varactor structure

There are several factors that influence the response time of a varactor. The most important is RC time constant. The ON-capacitance ($C_{ON}$) and the resistance ($R_{ON}$) of the

load form the RC time constant. The RC time constant is given by $\tau_{RC} = R_{ON} C_{ON}$. When the MIS varactor switch is turned ON or OFF, both the capacitance and resistance changes. To estimate the upper limit of the RC time constant, maximum values are used which corresponds to ohm state. While simulating MIS varactor, the measured ON-capacitance ($C_{ON}$) is 2.26e-12 F which is the highest capacitance of the switch when applied bias is equal to zero. Whereas the resistance ($R_{ON}$) is calculated with the other parameters obtained from the simulation as shown below.

$$R = R_{SH} \times \left(\frac{L}{W}\right)$$

Length = $(0.3 \times L_{SCH}) + (L_{GAP1}) + (L_{MIS2}) + (L_{GAP2}) + (0.3 \times L_{MIS2}) = 3.6$ μm; Width = 1mm

Length involved in calculating resistance during the ON state of the MIS varactor is depicted in the Fig. 4.2.
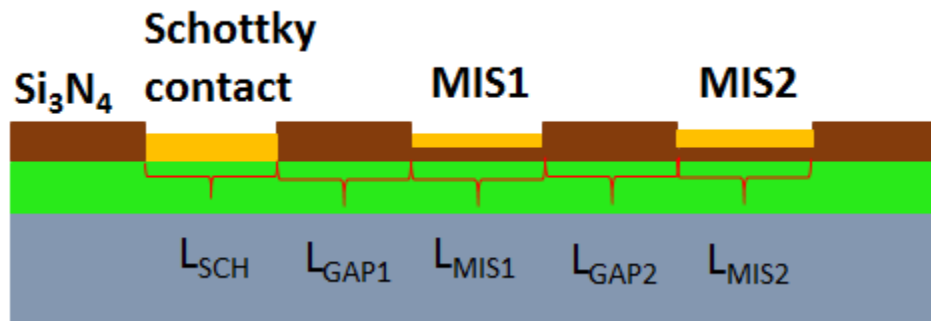


Figure 4.2 Zoomed in figure of the device structure showing the length of metal contact and electrode spacing

$$R_{ON} = 310 \times \left(\frac{3.6}{1000}\right) = 1.116 \, \Omega$$

Resistance ($R_{ON}$) = 1.116 Ω where $R_{ON}$ is the impedance of the transmission line where the switch is connected or the load, $R_{SH}$ is sheet resistance is estimated as 310 Ω/sq, L is Length, W is Width.

$$\tau_{RC} = R_{ON} \times C_{ON} = 2.522^{-12} \text{ s}$$

This $\tau_{RC}$ calculated using $R_{ON}$ and $C_{ON}$ is an intrinsic time constant value which is theoretically achievable with this MIS varactor. In reality the MIS varactor electrodes are connected to 50 Ohm transmission line as shown in the Fig. 4.3.
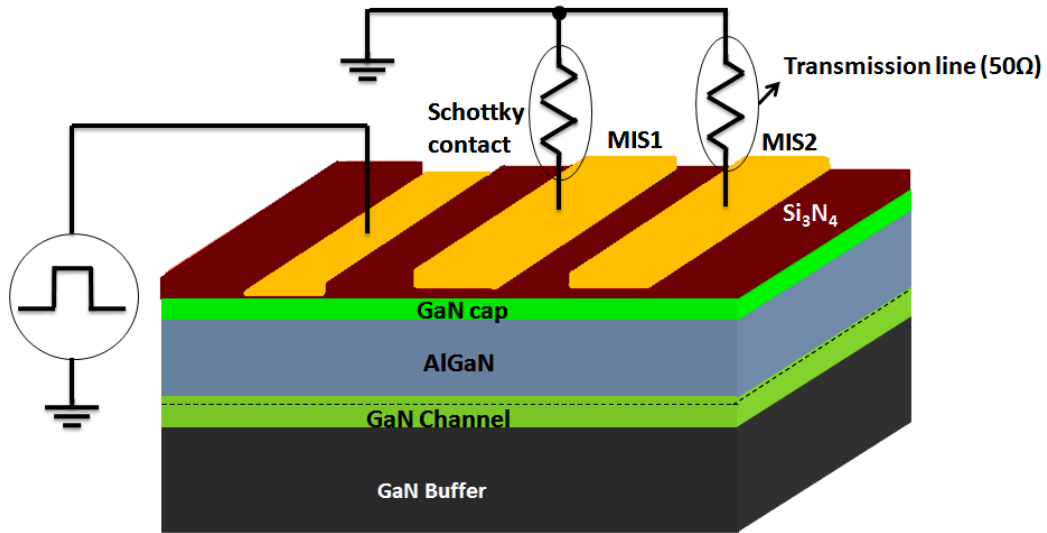


Figure 4.3 Circuit layout of MIS varactor switch

The time constant for this circuit which includes the transmission line with the MIS varactor can be estimated as follows,

$$\tau_{RC} = (R_{ON} + R_{TL}) \times C_{ON} = (1.116 + 50) \times 2.26e\text{-}12 = 115.522e\text{-}12 \text{ s}$$

The capacitance of the varactor must be kept small to prevent the RC time constant from limiting the response time. Trade-offs between fast transit times and low

44

capacitance are necessary for high-speed response. In the OFF state, the conduction channel is depleted (pinched-off), which causes the MIS varactor to exhibit very high resistance ($R_{ON}$), mechanism which provides good isolation at low frequencies. In reality the actual switching speed might vary from ideal value because every switch has some parasitic capacitance, inductance, resistance, and conductance. These parasitic components combine to degrade the speed of response of the switch. To verify the estimated RC time constant value of the MIS varactor, transient simulations were carried out using the Sentaurus software.

For the Sentaurus simulations, study of transient response measured the internal time constant of the device without any involvement of the external circuit. This enabled the actual semiconductor device to be simulated instead of mixed mode. Sentaurus Device computes the transient response of the MIS varactor to a voltage signal. Duration of the input pulse is specified according to which the physical device equations are solved consistently. A transient simulation is performed for the time duration specified in the "Transient" command. In that command, the start time, final time, and step size constraints (initial, maximum, minimum) are in seconds. Actual step sizes are determined internally, based on the rate of convergence of the solution at the previous step. "Increment" command determines the maximum step size increase [7]. Simulation results are plotted automatically using the Inspect and it consists of transient response of the output voltage, total current under MIS electrode through the n-channel with overlaying the input pulse. "Time" command is used in the simulation to print the time in the transient response plot [7]. For the MIS varactor time dependent boundary conditions are

45

specified along with the list of voltage-time pairs. The voltage is ramped up to -10V from 0V and a double pulse is created.

Electrode {

{ Name="MIS1"   Schottky Workfunction= 4.4 voltage = (0 at 0, 0 at 30e-9,-10 at 90e-9,-10 at 90e-9,0 at 120e-9,0 at 150e-9,0 at 180e-9, 0 at 210e-9,-10 at 240e-9,-10 at 270e-9,0 at 300e-9,0 at 330e-9)}

{ Name="MIS2"   Schottky Workfunction= 4.4 voltage = (0 at 0, 0 at 30e-9,-10 at 90e-9,-10 at 90e-9,0 at 120e-9,0 at 150e-9,0 at 180e-9, 0 at 210e-9,-10 at 240e-9,-10 at 270e-9,0 at 300e-9,0 at 330e-9)}
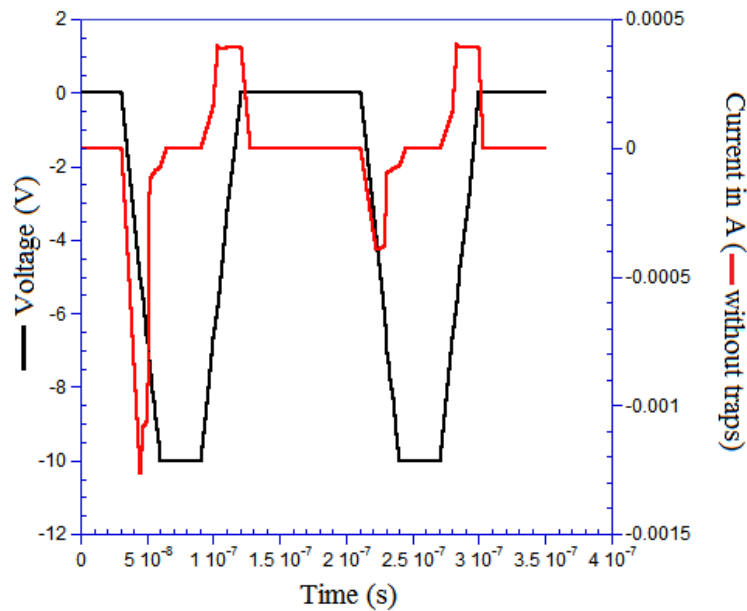
}



Figure 4.4 Simulated transient response of the MIS varactor switch.

Simulation of transient response in Sentaurus had issues in charactering the speed of switching because varactor does not have any current flowing through the channel. One of the approach is to monitoring capacitance as a function of time during transient. However this complicates the simulation because it requires AC signal and the pulse signal to be applied at the same time which results in convergence issues. As an alternative approach, current flowing through the gate is traced. In steady state this current is zero and whenever this current is not zero there exists a transient. Transient plot of MIS varactor is exactly like biased RC circuit. The current is zero before the ramp starts and also zero after the ramping is over. DC current does not flow through the capacitor. During the ramping, there is a current through capacitor according to i = C*dV/dt. So the square wave response is observed. The total current curve does not resemble the exact shape of the square waveform because in real device, on top of this theoretical response there is a component related to internal charging-discharging of varactor components.

## 4.2. Transient response in presence of defects

In hetero-structures, a junction formed with two different materials of different lattice constant suffers inherent stress which leads to the formation of point defects and threading dislocations which appear as traps. In the semiconductors, traps act like "trapping center" for mobile charges in the region of defects. Effect of traps and self-heating on the current transient response and the contribution of each factor is crucial for the optimization of the performance of AlGaN/GaN HEMTs [8]. Studies that include both effects in the current transient response simulation are still lacking. Generally in HEMTs, the switching speed is strongly influenced by the traps that are present in the

47

bulk and the surface trapping mechanisms. A donor type trap is positively charged (ionized) when empty and neutral when filled with an electron. An acceptor type trap is neutral when empty and negatively charged (ionized) when filled with an electron. In general the GaN bulk is filled with acceptor traps [8]. Electrons in the channel tunnel into neighboring interface or they are injected into the buffer and get trapped in it by deep level traps very quickly. Trapping of electrons lowers its energy. There is a preferable path for electron going from higher energy to lower energy. Retrieving these trapped electrons to conduction band is in slower process because the probability of escaping from deep traps levels is relatively low. Depending upon the type of trap, level and concentration of traps the escaping time varies from millisecond to seconds. This is the main reason to simulate the transient response plots in the presence of deep traps in the GaN buffer layer. For the study of trap behavior, different type of traps along with various concentrations and positions of traps were simulated. Fig. 4.5 shows the measured transient response of the MIS varactor switch with and without traps. For this plot, acceptor traps are used in GaN buffer layer. Its concentration is 1e16 cm^-3 and its position is 0.3eV form the Conduction Band.
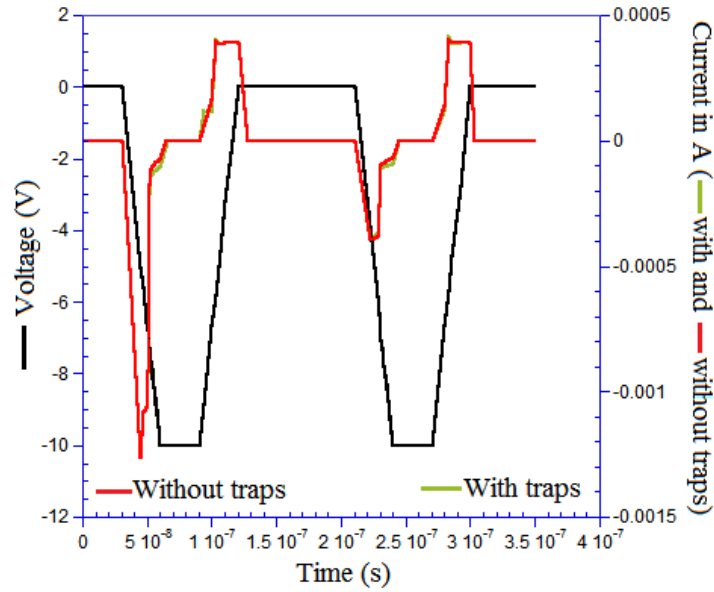
48

Figure 4.5 Simulated transient response (with and without traps)

The response in the transient plots for the MIS varactor with the presence of the traps is nearly the same as in ideal device without any defects. The reason for that is that, the defects in GaN materials have very high activation energy and therefore it takes significant time for those defects to charge - discharge. This time is typically in ms - second range and is therefore much longer than the typical turn on - turn off times. Therefore, during the transient, the charge state of defects does not change and their effect on transient is minimal. This makes the varactor a really fast device.

Actual effect of the traps is prominent in the eDensity profile of the device with increase in the negative bias applied to the electrodes. The snapshots of the eDensity profile at various time during the entire transient simulation is shown in the Fig. 4.6.
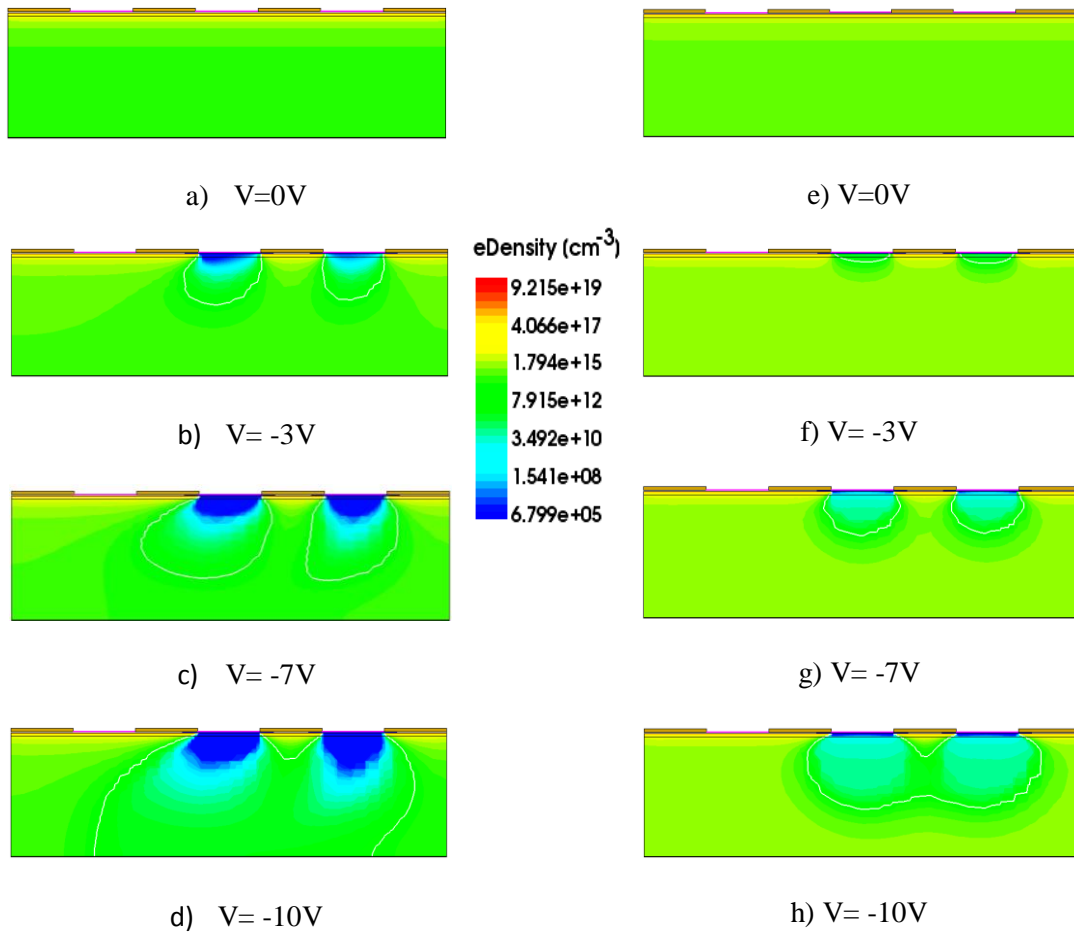
49

Figure 4.6 eDensity profile of MIS Varactor (with &without traps) during transient response with varying bias conditions

In the above Fig. 4.6, images (a) to (d) represent the snapshots of eDensity profile of MIS varactor without any traps added to it with increasing negative bias (from 0V to -10V) applied to the control electrode. Whereas images from (e) to (h) represent the eDensity profile with acceptor traps added to the GaN buffer layer at similar biasing conditions as that of without traps. This clearly depicts the depletion of 2DEG with increasing negative bias.

The experimentally measured switching characteristic of the varactor switch is shown in Fig.4.7. The measurements were done on wafer using the probe station. The pulsed

50

control voltage was generated using HP 8011A pulse generator and switching response was observed using a Tektronix TDS 2022C oscilloscope [6]. The signal from the pulse generator biased the varactors via the coaxial cable connected to the probes. The RF signal was applied at 2 GHz frequency and the signal amplitude was 0 dBm. The pulsed voltage amplitude was applied in the range from 10-15V. The limitations imposed by the cable capacitances limited the achievable rise/fall time to around $0.8 - 0.9$ μs [6]. As seen from Fig 4.7, the varactors do not add any delay to the input pulses
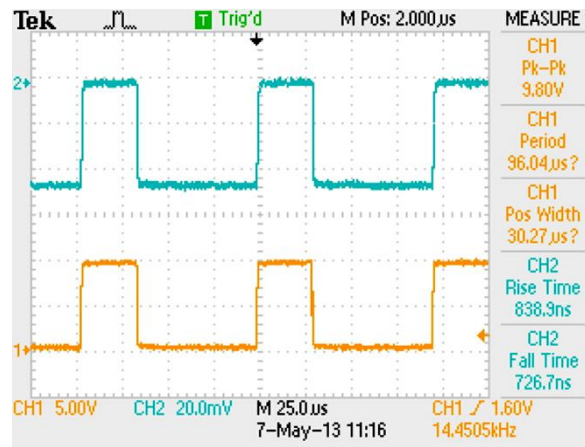


Figure 4.7 Switching time of Schottky C3 varactor Switch; yellow line-applied pulsed control voltage; blue line-Turn ON (fall time) and Turn OFF (rise time) times

The estimates show that varactor based switch response time is well below 0.1 μs [6]. The on-wafer measurements would not allow to resolve the nanosecond or sub nanosecond rise/fall time due to parasitic parameters of probes and connecting cables. In the future work it would be interesting and important to characterize the switching time of varactor using RF packages with minimized parasitic parameters.

51

# CHAPTER 5

## CONCLUSION

In this work, we studied a novel type of RF switch based on III-Nitride varactor. Unlike HEMTs, varactor uses capacitance modulation to control the flow of RF signal and offers a number of advantages over HEMTs: they allow for shorter channel, do not have gates or ohmic contacts and hence the fabrication is alignment- and anneal - free, they do not consume DC current and provide the DC block. Unlike regular varactor diodes, in this work, we analyze three-terminal varactor having independent control electrode which further enhances the switch performance.

RF switch analysis of the MIS varactor is done by modeling and simulation using Synopsys Sentaurus tools and MATLAB. CV characterizations were performed and the obtained results are compared with available experimental data of two terminal C3 varactor. We were able to get isolation of 30dB at 18 GHz for the MIS varactor whereas C3 was able to achieve only 25dB at 18 GHz. This is possible because the Sentaurus simulated three terminal MIS varactor OFF capacitance is much lower than the experimentally measured two terminal OFF capacitance. This low OFF capacitance is possible in three terminal MIS varactor because both the MIS electrodes are depleted simultaneously in the OFF state which leads to very low capacitance whereas in two terminal C3 varactor out of the two electrodes only turns OFF and the other remains ON (only one electrode is depleted and the other is accumulated). Hence the series

52

capacitance of the two electrodes remains high which leads to higher OFF capacitance values when compared to three MIS varactor.

Modeling approach allows obtaining device characteristics and material dependencies that are hardly achievable in experiments, such as effect of donor and acceptor traps. Acceptor traps were simulated in the GaN buffer layer and its effect on the switch performance characteristics were studied. Peak capacitance or the ON capacitance values are nearly not affected by traps whereas the OFF capacitance is marginally affected by the traps. MIS varactor device uses CV dependence to achieve switching as opposed to I-Vs used in HEMT device for the same purpose. The C-V dependence is expected to be affected by traps much weaker than the I-V. Therefore the varactor performance is less vulnerable to the defects than that of HEMT.

Transient response is demonstrated with nanosecond response where results were in agreement with the theoretical prediction. The response in the transient plots for the MIS varactor demonstrated good stability with the presence of the traps. The reason for that is that, the defects in GaN materials have very high activation energy and therefore it takes significant time for those defects to charge - discharge. This time is typically in ms - second range and is therefore much longer than the typical turn on - turn off times. This makes the varactor a really fast device. In overall the proposed three terminal MIS varactor promises significant performance improvements over the existing two terminal C3 device. In the future work it would be interesting and important to fabricate and characterize the varactor device using RF packages with minimized parasitic parameters.

## REFERENCES

[1] Khan, Muhammad Bilal. *Third order nonlinearity in III-nitride microwave switches*. Diss. UNIVERSITY OF SOUTH CAROLINA, 2011.

[2] Simin, G., et al. "Novel approaches to microwave switching devices using nitride technology." *International Journal of High Speed Electronics and Systems* 20.01 (2011): 219-227.

[3] Wang, Jingbo. *High-performance gateless III-nitride microwave switches*. Diss. University of South Carolina, 2010.

[4] Jahan, Faisal. "High Performance RF Control Devices Using Capacitively Coupled Contacts (C3) Over III-N Heterostructures." (2013).

[5] YANG, YI-HSUAN. "Electromagnetic Modeling of GaN Varactor Microwave Switches." (2013).

[6] Gaevski, Mikhail, et al. "GaN microwave varactors with insulated electrodes." *physica status solidi (c)* 11.3-4 (2014): 853-856.

[7] Guide, Sentaurus Device User. "Version H-2013.03." *Synopsys, Mountain View, CA, USA* (2013).

[8] Miccoli, Cristina, et al. "Trapping and thermal effects analysis for AlGaN/GaN HEMTs by means of TCAD simulations." *IEEE Electron Device Letters* 34.9 (2013): 1121-1123.

[9] Charbonniaud, C., et al. "Electrothermal and trapping effects characterisation of AlGaN/GaN HEMTs." (2003).